JOURNAL OF PROPULSION AND POWER
Vol. 23, No. 5, September–October 2007

Technical Notes

TECHNICAL NOTES are short manuscripts describing new developments or important results of a preliminary nature. These Notes should not exceed 2500 words (where a figure or table counts as 200 words). Following informal review by the Editors, they may be published within a few months of the date of receipt. Style requirements are the same as for regular contributions (see inside back cover).

Burning-Rate Calculations of Wide-Distribution Ammonium Perchlorate Composite Propellants

Muhammad Mazhar Iqbal* and Wang Liang†
Northwestern Polytechnical University, 710072 Xi'an, People's Republic of China

DOI: 10.2514/1.23748

Nomenclature

A_{fh}	=	average flame-height factor with respect to the oxidizer
A_s	=	kinetic prefactor for surface decomposition
B_{fh}	=	average flame-height factor for the binder
b	=	characteristic surface dimension
c_g	=	specific heat capacity of the oxidizer combustion gases
c_s	=	specific heat capacity of the solid
D_{ox}	=	oxidizer particle size
E_s	=	activation energy for surface decomposition
k	=	rate constant
m	=	mass flow rate
O/F	=	oxidizer/binder ratio
P	=	pressure
Q	=	heat released in the flame
Q_{fuel}	=	heat of the binder decomposition
Q_L	=	net heat released at the oxidizer surface
R	=	molar gas constant
r	=	burning rate
S	=	surface area
T_{ox}	=	oxidizer monopropellant flame temperature
T_s	=	surface temperature
T_0	=	initial propellant temperature
X_D	=	diffusion-flame height
X^*	=	flame standoff distance
α	=	mass fraction in the propellant
β_F	=	fraction of the oxidizer that reacts in the diffusion flame to heat the oxidizer
β_{ox}	=	fraction of the oxidizer that is used to heat the oxidizer
β_p	=	fraction of the oxidizer not involved in the condensed phase reaction
ΔH_s	=	latent heat of the solid oxidizer
δ	=	flame reaction order
λ_g	=	gas thermal conductivity
ξ	=	dimensionless flame height
ρ	=	density

Subscripts

b	=	associated with the binder
j	=	number of the oxidizer particle-size fraction in the propellant
ox	=	associated with the oxidizer
PF	=	associated with the primary flame
p	=	associated with the propellant
0	=	represents the total or initial conditions

Presented as Paper 1161 at the 44th AIAA Aerospace Sciences Meeting and Exhibit, Reno NV, 9–12 January 2006; received 9 March 2006; revision received 13 March 2007; accepted for publication 30 March 2007.

*Research Scholar, College of Astronautics.
†Professor, College of Astronautics.

I. Introduction

AMMONIUM perchlorate (AP) used in composite propellants consists of various blends of particle sizes for high loading density and stable combustion. Three or four particle sizes are commonly used in propellants, which are sufficient to come close to a viscosity optimum for a specific solid loading. Most of the practical propellant formulations have a wide-distribution multimodal oxidizer blend containing both very large (200 to 400 μm) and very small (1 to 25 μm) AP particles. The oxidizer particle size and particle-size distribution of various blends of oxidizer have a considerable effect on the burning rate of the propellant. The general need is to describe the burning rate of these propellants in terms of oxidizer particle-size distribution. The objective of this research is to describe a combustion model for the determination of burning rates and combustion properties for multimodal AP composite propellants.

Combustion models based on the multiple-flames concept, such as the Beckstead–Derr–Price (BDP) model [1], petite ensemble model (PEM) [2], Cohen and Strand model [3], and Beckstead models [4–6], have been able to predict the ballistic properties (burning rate and pressure exponent) of various polydisperse propellants to within about 10%. These models seek to simplify the statistically three-dimensional propellant geometry by unimodal oxidizer particles of a representative size surrounded by some binder layer of an equivalent extent. The influence of the size distribution on the average burning rate is predicted by integrating the results of independent analysis of each particle size. These models, however, are not able to predict the burning-rate behavior of the wide-distribution propellants.

Wide-distribution propellants have unique combustion mechanisms at the propellant surface. Studies have shown that a thin layer of liquid binder covers portions of the exposed AP surface, which is a dominant combustion mechanism for wide-distribution solid propellants [7]. This binder covering reduces the oxidizer burning rate, and the difference in the measured and the predicted burning rates is related to the extent of oxidizer surface covered with binder. The oxidizer-to-fuel ratio in these propellants plays a dominant role in combustion. These considerations were accounted for while formulating the model for burning-rate calculations.

The basic modeling approach is based upon the BDP multiple-flames concept. The following changes were incorporated in the original model to achieve the objective:

1) The Price–Boggs–Derr (PBD) model [8,9] for AP deflagration is adopted with modified input parameters, which provides a realistic means for examining and understanding the self-deflagration properties associated with solid propellants. The model includes variable specific heat capacity and conductivity and describes self-deflagration as a function of pressure and initial temperature. As a result, the temperature and pressure dependence of burning rates of

composite propellants can better be predicted when compared with the previous models.

2) The oxidizer and binder are assumed with separate surface temperatures in the current model. Separate energy balances are taken for the oxidizer and binder to determine their respective surface temperatures.

3) The model is extended to incorporate the multimodal oxidizer sizes using a pseudopropellant approach following the Cohen and Strand model [3]. The burning rate of each pseudopropellant is calculated independently, using the monomodal model. The aggregate propellant burn rate is determined from all the mass flow rate and surface-area contributions of all the pseudopropellants.

II. Experimental Work

Ammonium perchlorate (oxidizer), hydroxyl-terminated polybutadiene (HTPB) (binder), aluminum (fuel), toluene diisocyanate (curing agent), and some common propellant additives were selected as the propellant ingredients for formulation experimentations. Three to four particle sizes of AP were used in varying proportions to study the effect on burning rate and pressure exponent. A sufficient quantity of all the raw materials was prepared and homogenized to ensure a uniform batch. A small-scale vertical mixer was used for mixing the propellant slurry and later the scale was enhanced to a larger mixer to observe the effect. Several mixes of propellant slurry were prepared to observe the effect of the formulation variables. Propellant slurry was cast in rectangular cartons under vacuum and cured at 70°C in an oven for three days. Samples were prepared from the cured propellant and were tested for burning rate, pressure exponent, temperature sensitivity of burning rate, and various mechanical properties (stress, strain, and modulus). The results obtained (statistical mean value of five test samples) from these tests are summarized and discussed next.

The effects of varying the mixing ratio of coarse and fine AP and the catalyst on propellant burning rates were studied. In the first step, trimodal AP compositions were varied but the total contents of AP remained unchanged. Three types of spherical and one type of nonspherical AP were used, referred to as types 1, 2, 3, and fine, respectively. The mass average diameters d_{43} of types 1, 2, and 3 were measured as 340, 250, and 135 μm, respectively. The average diameter d_{43} of the nonspherical (fine) AP was measured as 10 μm. The proportions of various AP fractions with the measured burning rate and pressure exponent are given in Table 1.

In formulations AH-101 and 104, types 1, 3, and fine AP were used. Formulation AH-105 was reproduced with the same compositions as that of no. 104, but replacing type 1 AP with type 2. This change resulted in increasing the burning rate and reducing the pressure exponent of the propellant, which is according to the expected trend. The rest of the propellant formulations were prepared by using type 2 AP as the coarse fraction. In formulations AH 106–108, the fine-AP proportion was increased from 5–25%, which was further increased up to 35% in formulation leading to no. AH-113. Formulation AH-110 was just the repetition of no. 108 to verify the results. A good reproducibility of the results was observed from nos. 108 and 110.

The results of the burning rate versus fine-AP contents are plotted and shown in Fig. 1. It can be seen from the figure that the burning rate rises with the increase in fine-AP contents. The rise becomes quicker when fine-AP contents are increased from approximately 20% onward. This effect is more clearly visible from Fig. 2, in which the mass average diameter d_{43} of the three AP fractions is plotted against the burning rate at 5.5 and 6.0 MPa.

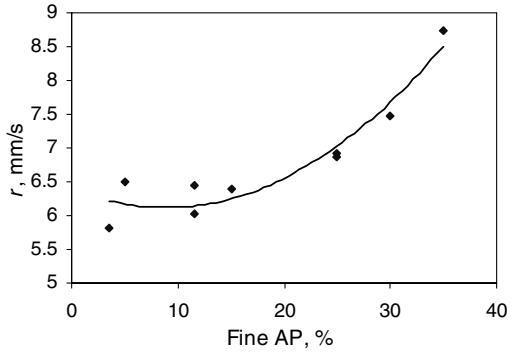

Fig. 1 Variation in propellant burning rate with fine AP.

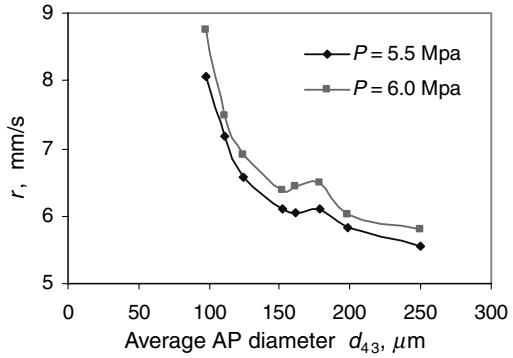

Fig. 2 Change in the burning rate with the AP mean diameter.

The burning rate decreases noticeably with d increasing, but at large d, the dependence of burning rate on d becomes weak. Such behavior of burning-rate dependence on d was also observed in previous studies with bimodal oxidizer at stoichiometric oxidizer/fuel ratios [10,11].

III. Combustion Mechanisms of Wide-Distribution AP Propellants

Wide distribution denotes a multimodal oxidizer blend containing both very large and very small oxidizer particles. The size difference allows higher levels of oxidizer-to-fuel ratio for the propellant to be achieved. The general need is to describe the burning rate of these propellants in terms of oxidizer particle-size distribution and binder composition. Combustion models based on the multiple-flames concept, such as BDP and the PEM, were able to predict the ballistic properties of previous polydisperse propellants to within about 10%.

Table 1 Various proportions of coarse and fine AP with burning rate and pressure exponent

Formulation code	AP, %				r (6.0 MPa), mm/s	Pressure exponent n
	Fine	Type 3	Type 2	Type 1		
AH-101	3.5	24.0	——	40.0	5.81	0.420
AH-104	11.5	28.0	——	28.0	6.02	0.398
AH-105	11.5	28.0	28.0	——	6.44	0.387
AH-106	5.0	31.5	31.0	——	6.49	——
AH-107	15.0	26.5	26.0	——	6.39	0.400
AH-108	25.0	21.5	21.0	——	6.93	0.430
AH-110	25.0	21.5	21.0	——	6.88	0.430
AH-112	30.0	19.0	18.5	——	7.48	——
AH-113	35.0	16.5	16.0	——	8.74	0.530

The influence of size distribution on the average rate is predicted by integrating the results of independent analysis of each particle size. These models, however, are not able to predict the burning-rate pressure dependence of wide-distribution propellants.

Comparison between measured and predicted burning rates from the previous studies are given in Fig. 3. Incrementally increasing the replacement of fine particles with the coarse particles in the trimodal AP propellant resulted in a decrease in measured burning rate. Results of PEM calculations are close to the measured burning rates at lower concentrations of coarse particles, but miss the decrease in rate as the coarse fraction is increased. Two possible phenomena that could cause this difference are 1) control of the ballistics by the fine-AP/HTPB (pocket propellant) matrix and 2) local intermittent burning related to the mass fraction of the coarse oxidizer particles. Because of the fuel-rich nature of the fine particle combustion, these propellants also exhibit extreme sensitivity to changes in binder composition.

Wide-distribution propellants have unique combustion mechanisms. The ballistic results of these propellants reveal anomalous burning rates. High-speed photographs and examination of extinguished propellant surfaces have shown evidence of molten liquid binder flowing on the propellant surface. This was indicated by the beads of binder flowing off the burning surface in the window-bomb movies and thin layers of binder covering portions of the oxidizer particles on the extinguished surface [7]. The binder flow increases significantly as the oxidizer-to-fuel ratio of the pocket propellant is lowered.

The binder covering reduces the oxidizer burning rate and is the main cause of differences between the predictions made with the PEM combustion model and the experimental results for wide-distribution propellants. The fraction of the AP burning surface covered with the molten binder determines the magnitude of the propellant burning-rate suppression. Experimental evidence suggests that lowering the oxidize-to-fuel ratio of the pocket propellant increases the binder-covering fraction. The binder-covering fraction also varies with the combustion pressure [12].

IV. Combustion Modeling

The combustion model is based on the BDP multiple-flames concept [1]. Separate surface temperatures for the oxidizer and binder were assumed following Beckstead and McCarty [5]. A complete description of the model is given in [13]. The key equations used in the model are summarized next.

A. Mass Flow Rates

The mass flow rates of the oxidizer and binder depend solely on their respective surface temperatures through the Arrhenius pyrolysis law. The mass flow rate of the oxidizer for a given surface temperature is calculated by

$$m_{\mathrm{ox}} = \rho_{\mathrm{ox}} r_{\mathrm{ox}} = A_{sox} \exp\left(\frac{-E_{sox}}{RT_{sox}}\right) \tag{1}$$

Similarly, the binder mass flow rate is given by

$$m_b = \rho_b r_b = A_{sb} \exp\left(\frac{-E_{sb}}{RT_{sb}}\right) \tag{2}$$

B. Separate Energy Balance for Oxidizer and Binder

The energy balance for the AP is written as

$$\begin{aligned} m_{\mathrm{ox}} S_{\mathrm{ox}}[c_s(T_{\mathrm{sox}} - T_\circ) + \Delta H_s + Q_L] \\ = \beta_{\mathrm{ox}}\beta_F(m_{\mathrm{ox}} S_{\mathrm{ox}} + m_b S_b) Q_{\mathrm{PF}} \exp(-\xi_{\mathrm{PFox}}) \\ + \beta_{\mathrm{ox}}(1-\beta_F) m_{\mathrm{ox}} S_{\mathrm{ox}} Q_{\mathrm{ox}} \exp(-\xi_{\mathrm{ox}}) \end{aligned} \tag{3}$$

The surface temperature of the oxidizer is calculated from the preceding equation and is given by

$$T_{sox} = T_\circ + \frac{\beta_{\mathrm{ox}}\beta_F(m_{\mathrm{ox}} S_{\mathrm{ox}} + m_b S_b) Q_{\mathrm{PF}} \exp(-\xi_{\mathrm{PFox}}) + \beta_{\mathrm{ox}}(1-\beta_F) m_{\mathrm{ox}} S_{\mathrm{ox}} Q_{\mathrm{ox}} \exp(-\xi_{\mathrm{ox}})}{c_s m_{\mathrm{ox}} S_{\mathrm{ox}}} - \frac{\Delta H_s + Q_L}{c_s} \tag{4}$$

Similarly, the energy balance for the binder is taken as

$$\begin{aligned} m_b S_b[c_s(T_{\mathrm{sb}} - T_\circ) + Q_{\mathrm{fuel}}] \\ = (1-\beta_{\mathrm{ox}})(m_{\mathrm{ox}} S_{\mathrm{ox}} + m_b S_b) Q_{\mathrm{PF}} \exp(-\xi_{\mathrm{PFb}}) \end{aligned} \tag{5}$$

Equation (5) is used to calculate the β_{ox} which is given by

$$\beta_{\mathrm{ox}} = 1 - \frac{m_b S_b[c_s(T_{\mathrm{sb}} - T_\circ) + Q_{\mathrm{fuel}}]}{(m_{\mathrm{ox}} S_{\mathrm{ox}} + m_b S_b) Q_{\mathrm{PF}} \exp(-\xi_{\mathrm{PFb}})} \tag{6}$$

C. Binder Regression Rate

The binder regression rate is calculated by continuity of the propellant:

$$m_b S_b = m_{\mathrm{ox}} S_{\mathrm{ox}} \left(\frac{\alpha_b}{\alpha_{\mathrm{ox}}}\right) \tag{7}$$

$$r_b = \frac{m_b}{\rho_b} \tag{8}$$

This regression rate is used in the surface-area calculations to determine S_{ox}. Unlike the BDP model, it is done in iteration, because r_b is function of S_{ox} in this calculation. The regression rate is then used to determine T_{sb} from Eq. (5).

D. Flame Heights

The BDP model used an approximation of the Williams and Burke–Schumann diffusion flame to determine an effective diffusion-flame height over the AP. The same basic approach is used for the calculations of the diffusion-flame height. However, a separate averaging method is applied to the diffusion-flame height over the oxidizer and binder.

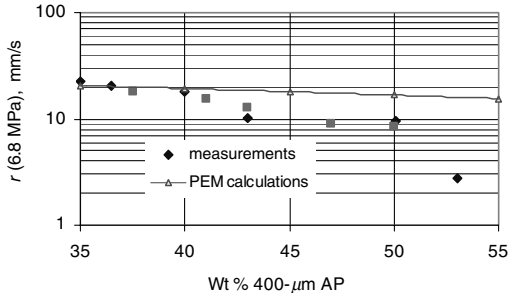

Fig. 3 Comparison of predicted and experimental measured burning rates.

The dimensionless flame height over the oxidizer is given by

$$\xi_{\mathrm{PFox}} = \frac{c_s m_p (X^*_{\mathrm{ox}} + X_{D\mathrm{ox}})}{\lambda_g} \tag{9}$$

$$X_{D\mathrm{ox}} = A_{\mathrm{fh}} \times X_D \tag{10}$$

The dimensionless flame height over the binder is given by

$$\xi_{\mathrm{PF}b} = \frac{c_s m_p (X^*_{\mathrm{PF}} + X_{Db})}{\lambda_g} \tag{11}$$

$$X_{Db} = B_{\mathrm{fh}} \times X_D \tag{12}$$

It turns out that the factor B_{fh} is much smaller than A_{fh}, the average flame-height factor with respect to the AP. Thus the binder is heated by a relatively close-in flame, which is consistent with Burke–Schumann model solutions for flames that extend over the fuel.

X^*_{PF} is calculated by the following relationship:

$$X^*_{\mathrm{PF}} = \frac{m_p}{k_{\mathrm{PF}} P^{\delta_{\mathrm{PF}}}} \tag{13}$$

Calculations of the diffusion-flame height X_D and the heat-release term used in Eqs. (4) and (6) are adopted from the BDP model and elaborated in [14]. The characteristic surface dimension b that is used to determine the diffusion-flame height X_D is different from the BDP model and is given later in this paper.

E. Multimodal Propellant Calculations

Several different approaches were used for building up the component modal contributions to express the aggregate propellant burning rate. The two most common approaches presented by Cohen and Strand [3] and Beckstead [6,10] were explored during this study. The original Cohen and Strand [3] modeling approach failed to calculate the burning rates of AP propellants having a wide distribution of particle sizes. In his later models, Beckstead [6,15] used a time-averaging approach, assuming that the propellant burns through alternate layers of binder and oxidizer at significantly different rates. The model gives good results for nitramine propellants associated with a significant ignition delay time. The Cohen and Strand [3] model is used for the purpose of present calculations, which gave good results with modifications described earlier.

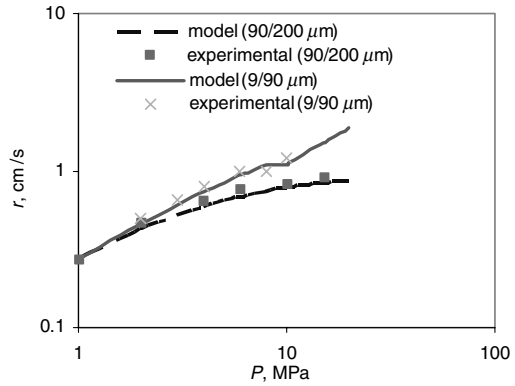

Fig. 4 Results of bimodal AP/HTPB propellants compared with the experimental data.

In the Cohen and Strand [3] approach, each modal component is viewed as a pseudopropellant. Each pseudopropellant includes an assigned portion of the binder. The burning rate is determined from all of the mass flow rate and surface-area contributions by serially building up pseudopropellant contributions:

$$m_{p,n} \sum_{1}^{n} S_{oj} = (m_{\mathrm{ox}} S_{\mathrm{ox}})_{j=n} + (m_b S_b)_{j=n} + m_{p,n-1} \sum_{1}^{n-1} S_{\mathrm{oj}} \tag{14}$$

$$r = \frac{m_{p,n}}{\rho_p} \tag{15}$$

The first two terms on the right side of Eq. (14) are the mass flow contributions of the oxidizer and the binder for last pseudopropellant. In the calculation procedure, $j = n$ represents the coarsest-particle-size pseudopropellant. The characteristic surface dimension b_j for multimodal propellant calculations is given by [5]

$$b_j = \frac{D_{\mathrm{ox}j}}{\sqrt{6}} \left[1 + \frac{\rho_{\mathrm{ox}}/\rho_b}{(O/F)_j} \right] \tag{16}$$

The parameter $(O/F)_j$ depends upon the apportioning of the binder to the oxidizer among the pseudopropellants. Cohen and Strand used a constant $(O/F)_j$ value in their model. This was changed and the effective O/F ratio for each pseudopropellant is assigned according to their relative proportion in the propellant. This approach affords the opportunity to predict more realistic burning rates and accounts for wide-distribution phenomena. The surface-area expressions used in the BDP mode are extended to incorporate the multimodal propellants.

Table 2 Experimental and calculated results for trimodal aluminized propellants

Formulation	AP proportions 10/135/250/340 μm	Burning rate,[a] mm/s		Pressure exponent[b]	
		Experimental	Calculated	Experimental	Calculated
AH-101	3.5/24/——/40	5.81	5.10	0.420	0.361
AH-104	11.5/28/——/28	6.02	5.58	0.398	0.358
AH-105	11.5/28/28/——	6.44	5.62	0.387	0.387
AH-106	5/31.5/31/——	6.49	5.28	——	——
AH-107	15/26.5/26/——	6.39	5.82	0.400	0.412
AH-108	25/21.5/21/——	6.90	6.38	0.430	0.485
AH-112	30/19/18.5/——	7.48	6.67	0.430	0.520
AH-113	3.5/16.5/16/——	8.74	6.96	0.530	0.562

[a]The pressure is 6.0 Mpa. [b]The pressure range is 4–10 MPa.

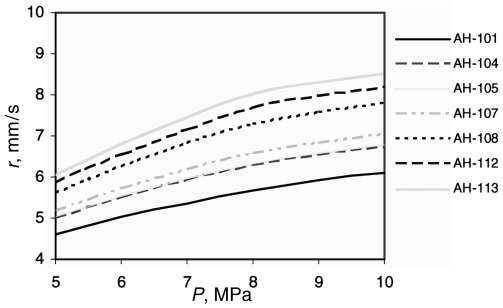

Fig. 5 Pressure dependence of the burning rate for trimodal AP/HTPB formulations.

V. Results and Discussions

Calculations are performed for a bimodal propellant and compared with the experimental data of King [16] and Miller [17,18] for the verification of the model. These propellants are good choices because they encompass a range of size distributions and AP concentrations. Calculation results are compared with experimental data of King's [16] formulation having 82% AP (90/200 μm, 1/5 ratio) and Miller's [17,18] formulation having 80% AP (9/90 μm, 1/1 ratio) and are shown in Fig. 4. The results show very good agreement with the data in both cases. A rise in the slope of 9/90 μm propellant curve is attributed to the shift from the diffusion-flame-control regime to AP flame control at about 10 MPa.

The model is extended to calculate the burning rates of wide-distribution particle sizes and aluminized propellants. Our own experimental data, which contain various formulation results of aluminized AP/HTPB propellants [19], are used for the calculations. These data are a good choice due to their versatile nature, having trimodal AP with variable particle sizes and proportions, and they provide the pressure exponent for most formulations. These data represent the real practical formulations. The results of burning rate and pressure exponent are compared and shown in Table 2. The calculated results are in very good agreement with the relevant experimental data. All of the results are within 20% deviation: 75% results lie within 15% deviation, and 50% calculations are within 10% deviation. The statistics shows the excellent predictions for such a practical wide-distribution aluminized propellant formulation. The pressure versus burning-rate curve for all the formulations of [19] are also plotted and shown in Fig. 5. This shows the good computational capability of the model with respect to both pressure and particle-size effects. Thus the desired purpose has been achieved.

All of the propellants were calculated at the initial temperature of 298 K. The effect of initial propellant temperature requires further work, which is still in progress.

VI. Conclusions

A model is presented for the combustion calculations of AP-based composite propellants within the framework of the BDP model. The model differs from the BDP model in the sense that it accounts for the latest PBD model for AP deflagration with modified parameters. A separate energy balance is assumed for the binder to calculate different surface temperatures of the oxidizer and binder. A pseudopropellant approach is used for extension of the model to multimodal AP propellants. New parametric values used in the PBD model enable more widened and more realistic surface-temperature calculations of oxidizer and better predictions of monopropellant rates. Burning-rate calculations for various monomodal AP/HTPB propellants were performed and compared with the experimental data. Results are in good agreement. Then the model is extended to multimodal propellants and results are compared for bimodal AP propellant formulations that again show good agreement with the data. Finally, the results are computed for the most practical propellant formulations containing aluminum and trimodal AP in a wide distribution of particle sizes. The results of burning rate and pressure exponent are in very good agreement with the experimental data. Results show the good capability of the model for determining the effect of both pressure and AP particle size. The dependence of burning rate on initial temperature is not computed in the present study and work on that is still in progress. Because the model predicts the combustion properties of practical propellant formulations to a reasonable accuracy, overall propellant optimization can be performed and, as such, significant gains can be reached by reducing the time and cost for new propellant formulation development.

References

[1] Beckstead, M. W., Derr, R. L., and Price, C. F., "A Model of Composite Solid Propellant Combustion Based on Multiple Flames," *AIAA Journal*, Vol. 8, Dec. 1970.

[2] Glick, R. L., "Distribution Functions for Statistical Analysis of Monodisperse Composite Solid Propellant Combustion," *AIAA Journal*, Vol. 14, Nov. 1976.

[3] Cohen, N. S., and Strand, L. D., "An Improved Model for the Combustion of AP Composite Propellants," *AIAA Journal*, Vol. 20, No. 12, Dec. 1982, pp. 1739–1746.

[4] Beckstead, M. W., Derr, R. L., and Price, C. F., "The Combustion of Solid Monopropellants and Composite Propellants," *Thirteenth Symposium (International) on Combustion*, Combustion Inst., Pittsburgh, PA, 1971, pp. 1047–1056.

[5] Beckstead, M. W., and McCarty, K. P., "Modeling Calculations for HMX Composite Propellants," *AIAA Journal*, Vol. 20, No. 1, Jan. 1982, pp. 106–115.

[6] Beckstead, M. W., "A Model for Solid Propellant Combustion," *Eighteenth Symposium (International) on Combustion*, Combustion Inst., Pittsburgh, PA, 1981, pp. 175–185.

[7] Frederick, R., Jr., and Osborn, J. R., "Ballistic Studies of Wide Distribution Propellants," 36th AIAA/ASME/SAE/ASEE Joint Propulsion Conference and Exhibit, Huntsville, Al., AIAA Paper 2000-3318, July 2000.

[8] Price, C. F., Boggs, T. L., and Derr, R. L., "The Steady State Combustion Behavior of Ammonium Perchlorate and HMX," 17th Aerospace Sciences Meeting, AIAA Paper 79-0164, Jan. 1979.

[9] Price, C. F., Boggs, T. L., and Derr, R. L., "The Modeling of Solid Monopropellant Deflagration," 16th Aerospace Sciences Meeting, AIAA Paper 78-219, Jan. 1978.

[10] Beckstead, M. W., "An Overview of Combustion Mechanisms and Flame Structures for Advanced Solid Propellants," 36th AIAA/ASME/SAE/ASEE Joint Propulsion Conference, Huntsville, Al, AIAA Paper 2000-3325, July 2000.

[11] Chakarvarty, S. R., Price, E. W., Sigman, R. K., and Seitzman, J. M., "Plateau Burning Behavior of Ammonium Perchlorate Sandwiches and Propellants at Elevated Pressures," *Journal of Propulsion and Power*, Vol. 19, No. 1, Jan.–Feb. 2003, pp. 56–65.

[12] Fredrick, R. A., "Wide Distribution Propellants," U.S. Air Force Rocket Propulsion Lab., Rept. AFAL-TR-88-073, Edward's AFB, CA, June 1988.

[13] Iqbal, M. M., and Liang, W., *Combustion Calculations of Multimodal Ammonium Perchlorate Composite Solid Propellants*, Theory and Practice of Energetic Materials, Vol. 6, Science Press, Beijing, China, 2005, pp. 1060–1068.

[14] Iqbal, M. M., and Liang, W., "Propellant Burning Rate Calculations with Improved Predictions," *Journal of Solid Rocket Technology*, Vol. 25, No. 1, 2002.

[15] Beckstead, M. W., and McCarty, K. P., "Modeling Calculations for HMX Composite Propellant," *AIAA Journal*, Vol. 20, No. 1, 1982, pp. 106–115.

[16] King, M. K., "A Model of the Effects of Pressure and Cross Flow Velocity on Composite Propellant Burning Rate," AIAA 15th AIAA/ASME/SAE/ASEE Joint Propulsion Conference, Las Vegas, NV, AIAA Paper 79-1171, June 1979.

[17] Miller, R. R., "Control of Solid Distribution in HTPB Propellants," U.S. Air Force Rocket Propulsion Lab., Rept. TR-78-14, Edward's AFB, CA, 1978.

[18] Miller, R. R., "Effects of Particle Size on Reduced Smoke Propellant Ballistics," 18th AIAA/ASME/SAE/ASEE Joint Propulsion Conference, Cleveland, OH, AIAA Paper 82-1097, 1982.

[19] Iqbal, M. M., and Liang, W., "Combustion Modeling and Formulation Design of Composite Solid Propellants—Experimental Study," *5th International Symposium on Multiphase Flow, Heat Mass Transfer and Energy Conversion* [CD-ROM], Xi'an Jiaotong Univ. Press, Xi'an, China, July 2005.

S. Son
Associate Editor